



A risk scoring system for predicting visceral pleural invasion in non-small lung cancer patients

Shuhei Iizuka¹ · Akikazu Kawase¹ · Hiroaki Oiwa¹ · Toshinari Ema¹ · Norihiko Shiya¹ · Kazuhito Funai¹

Received: 21 December 2018 / Accepted: 1 March 2019 / Published online: 19 March 2019
© The Japanese Association for Thoracic Surgery 2019

Abstract

Objective This study aimed to construct a simple scoring system for predicting visceral pleural invasion of non-small cell lung cancer (NSCLC) from computed tomography (CT) findings and clinicopathological factors in lesions directly under the pleural membrane.

Methods Among 376 cases of surgically treated NSCLC, cases in which the tumor was ≤ 7 cm in diameter and in contact with the pleura on the CT image were retrospectively extracted and examined. The CT findings and clinicopathological factors associated with the presence of pathological pleural invasion in each case were examined by Fisher's exact test. A score was then assigned based on the odds ratio obtained for each factor, and a risk scoring system for predicting pleural invasion was constructed.

Result In the 138 extracted cases, pathological visceral pleural invasion was found in 64 cases. The scoring system predicting pleural invasion could be defined as follows: pl risk score = 3 (tumor diameter in CT ≥ 24 mm) + 3 (tumor contact length with pleura in CT ≥ 16 mm) + 3 (smoking index ≥ 400) + 3 (clinically lymph node positive) + 2 (tumor with cavity in CT) + 2 (serum CEA level > 4.4 ng/mL). A score was calculated for each case and an ROC curve was created. The cutoff value was score 8 and the area under curve (AUC) was 0.68.

Conclusion Our findings suggest that visceral pleural invasion can be predicted using a score calculated from several simple CT findings and clinicopathologic factors.

Keywords Non-small cell lung cancer · Visceral pleural invasion · Risk scoring system · Prediction

Introduction

In non-small cell lung cancer (NSCLC), visceral pleural invasion is an aggressive and invasive factor [1, 2]. For example, pathological pleural invasion has been reported to occur significantly more frequently in patients with N2 and skip N2 metastasis [3, 4]. Predicting pleural invasion before surgery in individual patients would thus be useful for determining the stage and optimal treatment strategies. However, because it is difficult to predict visceral pleural invasion based on the imaging diagnosis, an accurate evaluation cannot be performed.

Subjects

The aim of this study was to construct a simple scoring system for predicting visceral pleural invasion of NSCLC from pretreatment image findings and clinicopathologic factors in case involving lesions directly under the pleural membrane.

Methods

In this retrospective study, among 376 NSCLC cases in our institution in which complete resection was performed from January 2012 to March 2017, those in which the clinically solid component of the tumor was ≤ 7 cm in diameter ($\leq cT3$) with the solid component in contact with pleura on preoperative computed tomography (CT) were extracted and examined. Cases in which preoperative induction therapy, including chest wall merger resection, were performed were excluded.

✉ Kazuhito Funai
kfunai@hama-med.ac.jp

¹ First Department of Surgery, Hamamatsu University School of Medicine, 1-20-1, Handayama, Higashi-ku, Hamamatsu, Shizuoka 431-3192, Japan

Contact between the solid component of the tumor and the pleura on CT was defined as follows: the solid component came in direct contact with the surface of the lung or interlobular pleura, the solid component of the tumor came in contact with the visceral pleura through a bundle-shaped pleural indentation sufficiently wide to be measured at the contact point.

The following CT findings were excluded from the definition: the solid component of the tumor came in contact with the visceral pleura through a linear pleural indentation (the width of which could not be measured at the contact point using CT), a ground glass component came in contact with the surface of the lung or the interlobular pleura, tumor infiltrating the chest wall.

We reviewed the medical records of all the extracted cases and analyzed the preoperative CT findings and clinicopathological factors associated with the presence of pathological pleural invasion. The following factors were examined as preoperative CT findings: tumor diameter, length of the area of contact between the tumor and the pleura (contact length), whether the tumor occurred in a usual interstitial pneumonia pattern (included in UIP pattern), whether the tumor was adjacent to a cavitory lesion (with cavity), whether the tumor was in contact with the pleura with a bundle-shaped pleural indentation defined as above, and whether the tumor was a contractile lesion characterized by the convergence of surrounding lung tissue or a bronchial vascular bundle. The following factors were examined as other preoperative clinicopathological factors: smoking index (S. I.) ≥ 400 , serum CEA level ≥ 4.4 ng/mL; and whether or not clinical lymph node metastasis was detected (cN1 or 0).

A receiver operating characteristic (ROC) curve was created for the presence of pathological pleural invasion according to the tumor diameter and contact length then cutoff values for each factor were determined. Fisher’s exact test was used to evaluate the relationships between the presence of pathological pleural invasion and the factors stated above. Based on each obtained odds ratio, the preoperative predictors were selected, and scores were assigned. Scoring was performed as follows: standardization with the smallest odds ratio set at 1.0 and recalculation of the other odds ratios. In addition, each recalculated value was doubled and rounded to the nearest integer. An ROC curve was then constructed, and a cutoff value was obtained for the total score of each case for predicting pleural invasion.

All statistical analyses were performed using the SPSS software program (version 25, IBM). *P* values of <0.05 were considered to indicate statistical significance. The authors A. Kawase and K. Funai were responsible for statistical analysis and interpretation. We defined complete resection as wedge resection or greater. Cases were clinically or pathologically staged based on the 8th Edition of the TNM Classification for Lung and Pleural Tumors. Histopathological examinations

were performed according to the World Health Organization criteria. We defined the presence of pathological pleural invasion as p11 or greater. The study protocol was approved by the institutional review board (reference number: 17–157).

Results

A total of 138 cases were extracted from the 373 cases. The patient characteristics are listed in Table 1. Pathological visceral pleural invasion was found in 64 cases (46%; p13, *n* = 5; p12, *n* = 14; and p11, *n* = 47).

Figure 1 shows the ROC curves of the tumor diameter and contact length for predicting the presence of pathological pleural invasion. Based on the ROC curve, the cutoff values of the tumor diameter and contact length were determined to be 24 mm and 16 mm, respectively.

The results of univariate analysis and the scores assigned for each preoperative factor are listed in Table 2. Based on the obtained odds ratio, scores were assigned to each factor. An odds ratio of 1.0–2.0 assigned a score of 2. Odds ratios of ≥ 2.0 were assigned a score of 3. Factors with odds ratios of < 1.0 were excluded from the risk factors for pleural invasion.

The pleural invasion (pl) risk score was determined as follows:

$$\begin{aligned} \text{pl risk score} = & 3(\text{tumor diameter} \geq 24 \text{ mm}) \\ & + 3(\text{tumor contact length} \geq 16 \text{ mm}) \\ & + 3(\text{S.I.} \geq 400) \\ & + 3(\text{clinically lymph node positive}) \\ & + 2(\text{tumor with cavity}) \\ & + 2(\text{CEA} > 4.4 \text{ ng/mL}). \end{aligned}$$

Table 1 Patient characteristics

Characteristics	No. of patients (%)	Median (range)
Age	138 (100)	73 (33–88)
Sex		
Male/female	106/32 (77/23)	
Smoking history		
Never smoker	28 (20)	
Smoker	110 (80)	
SI ≥ 400	99 (72)	
cT (UICC 8th)		
1a/1b/1c/2a/2b/2c	4/37/52/30/8/7 (3/27/38/23/6/5)	
Pathological pl		
p10/p11/p12/p13	72/47/14/5 (52/34/10/4)	
Histology		
Ad/Sq/LCNEC/others	90/33/6/9 (65/24/4/11)	

SI smoking index, pl pleural invasion, Ad adenocarcinoma, Sq squamous cell carcinoma, LCNEC large-cell neuroendocrine carcinoma

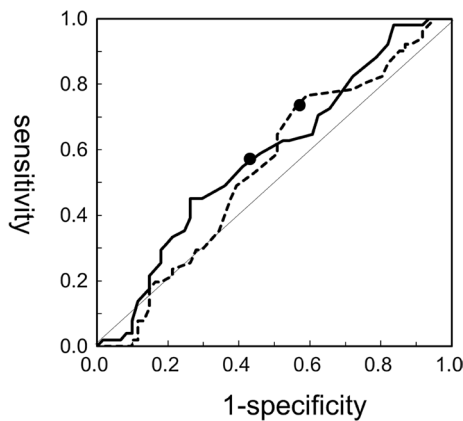


Fig. 1 The receiver operator characteristic (ROC) curves for the tumor diameter (dashed curve) and contact length (solid curve). The area under the curve values were 0.57 and 0.62, respectively. The cut-off values were 24 mm and 16 mm, respectively

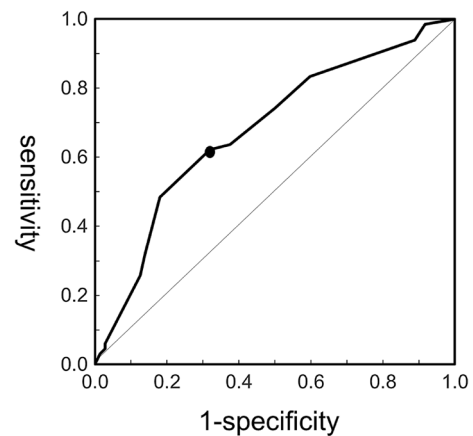


Fig. 2 The receiver operator characteristic (ROC) curve for the pleural invasion (pl) risk score. The area under curve was 0.68, and the pl cutoff value was score 8

The ROC curve of the pl risk score for predicting the risk of pleural invasion is shown in Fig. 2. The pl risk score showed moderate discrimination with an area under the curve (AUC) of 0.68. The cutoff value was score 8.

In Fig. 3, plots show the proportion of cases that actually had pathologic pleural invasion for each score value. Among the 138 analyzed cases, 64% of the cases with a score of ≥ 8 and 36% of the cases with scored of < 8 showed pathological pl positivity. The solid line in Fig. 3 is an approximate curve of the plots, showing the predicted risk of pl positivity according to each score value.

Discussion

The lymphatic vessels beneath the pleura do not pass through the hilar lymph nodes and flow directly into the mediastinum [5], which causes skip N2 metastases. Since visceral pleural invasion is independently associated with

skip N2 metastasis [5], the prediction of visceral pleural invasion is important for determining the stage and treatment strategies for NSCLC. Even in the clinical stage IA1 cases, where limited surgery may be considered, in cases in which visceral pleural invasion is suspected, it is necessary to select a surgical procedure with the existence of Skip N2 metastasis in mind. Furthermore, the relationship between pleural invasion and occult N2 can also be an important concern. Conversely, even in the cases without lymph node metastasis, pleural invasion has been shown to be associated with a worse prognosis [2, 6]. Thus, it is very important to accurately predict pleural invasion before surgery. For clinicians, however, it is a difficult task to predict the pleural invasion from pretreatment imaging findings and various clinical factors. We showed that visceral pleural invasion can be easily predicted by combining simple pretreatment factors, including a number of CT findings that cannot individually predict pleural invasion.

Table 2 The results of the univariate analysis and the score assigned for each preoperative factor

Preoperative factors	No. of patients (%)	Odds ratio	<i>p</i> value	95% C.I.	Score
CT findings of tumor					
Diameter ≥ 24 mm	80 (58)	2.3	0.03	1.07–4.82	3
Contact length ≥ 16 mm	58 (42)	2.1	0.04	1.01–4.48	3
Included in UIP pattern	17 (12)	1.0	1.0	0.30–3.03	–
With cavity	23 (17)	1.5	0.4	0.56–4.21	2
With bundle shape pleural indentation	26 (19)	0.8	0.7	0.29–1.95	–
Contractile lesion	78 (57)	0.7	0.3	0.33–1.40	–
SI ≥ 400	99 (72)	2.3	0.04	1.00–5.46	3
CES > 404 ng/mL	61 (44)	1.4	0.4	0.67–2.89	2
Clinically lymph node positive	13 (9)	2.7	0.1	0.70–12.5	3

SI smoking index

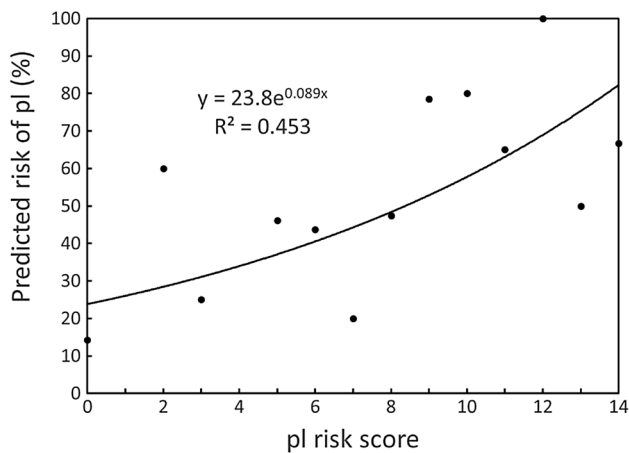


Fig. 3 Dots show the proportion of cases that actually had pathologic pleural invasion for each pl risk score value. The predicted risk of pl positivity according to each score value was shown with a solid line

The form of the lesion analyzed by 3-dimensional CT [7, 8], the maximum standardized uptake value (SUV max) of tumor on ^{18}F -FDG PET/CT [9], whether or not the lesion is GGN [10], and finding of dynamic MRI [11] have previously been reported to predict the pleural invasion of lung cancer. No studies have used a score calculated from multiple factors to predict visceral pleural invasion. In addition, the present scoring system can predict visceral pleural invasion using variables that are simple and low cost to obtain without the need for special equipment or software.

We believe that better scoring systems can be constructed by refining the preoperative factors through the evaluation of further cases in the future.

Conclusion

The result of the present study suggested that visceral pleural invasion in NSCLC can be predicted before treatment using several easily determined CT findings and clinicopathological factors.

Compliance with ethical standards

Conflict of interest The authors have declared that no conflict of interest exists.

References

1. Kawase A, Yoshida J, Miyaoka E, Asamura H, Fujii Y, Nakanishi Y, et al. Visceral pleural invasion classification in non-small-cell lung cancer in the 7th edition of the tumor, node, metastasis classification for lung cancer: validation analysis based on a large-scale nationwide database. *J Thorac Oncol*. 2013;8:606–11.
2. Jiang L, Liang W, Shen J, Chen X, Shi X, He J, et al. The impact of visceral pleural invasion in node-negative non-small cell lung cancer: a systematic review and meta-analysis. *Chest*. 2015;148:903–11.
3. Manac'h D, Riquet M, Medioni J, Le Pimpec-Barthes F, Dujon A, Danel C. Visceral pleura invasion by non-small cell lung cancer: an underrated bad prognostic factor. *Ann Thorac Surg*. 2001;71:1088–93.
4. Gorai A, Sakao Y, Kuroda H, Uehara H, Mun M, Ishikawa Y, et al. The clinicopathological features associated with skip N2 metastases in patients with clinical stage IA non-small-cell lung cancer. *Eur J Cardiothorac Surg*. 2015;47:653–8.
5. Imai K, Minamiya Y, Saito H, Nakagawa T, Ito M, Ono T, et al. Detection of pleural lymph flow using indocyanine green fluorescence imaging in non-small cell lung cancer surgery: a preliminary study. *Surg Today*. 2013;43:249–54.
6. Tian D, Pei Y, Zheng Q, Zhang J, Li S, Wang X, et al. Effect of visceral pleural invasion on the prognosis of patients with lymph node negative non-small cell lung cancer. *Thorac Cancer*. 2017;8:97–105.
7. Ebara K, Takashima S, Jiang B, Numasaki H, Fujino M, Tomita Y, et al. Pleural invasion by peripheral lung cancer: prediction with three-dimensional CT. *Acad Radiol*. 2015;22:310–9.
8. Kuriyama K, Tateishi R, Kumatani T, Kodama K, Doi O, Hosomi N, et al. Pleural invasion by peripheral bronchogenic carcinoma: assessment with three-dimensional helical CT. *Radiology*. 1994;191:365–9.
9. Tanaka T, Shinya T, Sato S, Mitsuhashi T, Ichimura K, Soh J, et al. Predicting pleural invasion using HRCT and ^{18}F -FDG PET/CT in lung adenocarcinoma with pleural contact. *Ann Nucl Med*. 2015;29:757–65.
10. Ahn SY, Park CM, Jeon YK, Kim H, Lee JH, Hwang EJ, et al. Predictive CT features of visceral pleural invasion by T1-sized peripheral pulmonary adenocarcinomas manifesting as subsolid nodules. *AJR Am J Roentgenol*. 2017;209:561–6.
11. Akata S, Kajiwara N, Park J, Yoshimura M, Kakizaki D, Abe K, et al. Evaluation of chest wall invasion by lung cancer using respiratory dynamic MRI. *J Med Imaging Radiat Oncol*. 2008;52:36–9.

Publisher's Note Springer Nature remains neutral with regard to jurisdictional claims in published maps and institutional affiliations.